Supporting Information For:

Mechanofluorochromic properties of β-iminoenolate boron complexes tuned by the electronic effects of terminal phenothiazine and phenothiazine-*S*,*S*-dioxide

Zhenqi Zhang, Zhu Wu, Jingbo Sun, Boqi Yao, Gonghe Zhang, Pengchong Xue and Ran Lu*

State Key Laboratory of Supramolecular Structure and Materials, College of Chemistry,

Jilin University, Changchun 130012, P. R. China

Tel: +86-431-88499179

E-Mail: luran@mail.jlu.edu.cn

Table S1. Photophysical data of **P2B**, **P16B**, **PO2B** and **PO16B**.

	Solvent	E_T (30) (kcal/mol)	λ_{abs} (ε^a) (nm)	λ_{em} (nm)	Stokes shift (cm^{-1})	$\Phi_F{}^b$
P2B	Cyclohexane	30.9	279(15075) 312(19527) 423(29008)	501	3681	0.58
	Toluene	33.9	310(17479) 424(27126)	541	5101	0.45
	THF	37.4	314(14263) 419(27789)	575	6475	0.30
	DCM	40.7	308(13269) 422(23524)	600	7030	0.20
	DMF	43.2	277(11928) 303(14916) 419(24358)	615	7606	0.03
	DMSO	45.1	310(12443) 421(24900)	628	7829	0.03
P16B	Cyclohexane	30.9	279(12563) 311(17393) 422(27522)	507	3973	0.57
	Toluene	33.9	311(15050) 422(25676)	539	5144	0.45
	THF	37.4	279(14808) 304(16490) 416(26405)	577	6707	0.29
	DCM	40.7	279(13269) 306(16496) 421(24804)	600	7086	0.23
	DMF	43.2	277(14071) 302(16536) 423(27804)	618	7459	0.07
	DMSO	45.1	276(13172) 302(15285) 418(24091)	632	8100	0.08
PO2B	Toluene	33.9	297(12531) 330(12011) 397(39232)	436 459	3402	0.24
	THF	37.4	296(23243) 324(16504) 393(53004)	454	3419	0.35
	DCM	40.7	296(12266) 327(12440) 393(42105)	455	3467	0.29

	DMF	43.2	296(21545) 326(15924) 392(57578)	461	3949	0.54
	DMSO	45.1	296(21284) 394(70738)	464	3829	0.70
PO16B	Cyclohexane	30.9	300(11305) 330(8961) 396(24320) 415(17470)	426 451	3080	0.16
	Toluene	33.9	300(12867) 330(11287) 397(33789)	436 459	3402	0.23
	THF	37.4	296(22174) 324(15608) 393(48463)	457	3563	0.34
	DCM	40.7	296(11104) 327(11494) 394(37883)	457	3499	0.31
	DMF	43.2	295(17114) 326(11999) 393(43894)	461	3949	0.55
	DMSO	45.1	297(13732) 394(45148)	464	3829	0.65

[a] $M^{-1}cm^{-1}$; [b] The fluorescence quantum yield (Φ_F) of **P2B**, **P16B**, **PO2B** and **PO16B** using 9,10-diphenylanthracene in benzene (Φ_F = 0.85) as standard.

Table S2. Fluorescence lifetimes of **P2B**, **P16B** and **PO2B** in solutions and in solid states.

sample	state	wavelength (nm)	lifetime (ns)
P2B	solution in cyclohexane	541	4.58
	as-synthesized crystal	531	2.52
		680	3.85
	ground powder	605	4.58
	fumed sample	548	2.93
	heated sample	526	2.64
P16B	solution in cyclohexane	539	4.70
	as-synthesized crystal	534	2.52
	ground powder	582	4.71
	fumed sample	540	2.99
	heated sample	544	3.66
PO2B	solution in toluene	449	0.59
		466	0.54
	as-synthesized crystal	545	6.49
	ground powder	518	4.72
	fumed sample	541	6.61

Table S3. Calculated absorption wavelengths λ_{abs} [nm], excitation energies E_x [eV], oscillator strengths f and dominant excitation character of **P2**.

λ [a] (nm)	E_x	f [b]	Composition
498.26	2.4884	0.2166	HOMO→LUMO (97%)
408.83	3.0327	0.0077	HOMO→LUMO+1 (92%)
			HOMO→LUMO+2 (5%)
360.01	3.4439	0.1363	HOMO-1→LUMO (63%)
			HOMO-1→LUMO+1 (3%)
			HOMO→LUMO+2 (31%)
350.47	3.5377	0.4256	HOMO-1→LUMO (28%)
			HOMO-1→LUMO+1 (2%)
			HOMO→LUMO+1 (6%)
			HOMO→LUMO+2 (59%)
322.04	3.8500	0.1170	HOMO-2→LUMO (45%)
			HOMO-1→LUMO+1 (18%)
			HOMO→LUMO+2 (2%)
			HOMO→LUMO+3 (4%)
			HOMO→LUMO+4 (25%)
315.63	3.9281	0.0486	HOMO→LUMO+3 (82%)
			HOMO→LUMO+4 (10%)

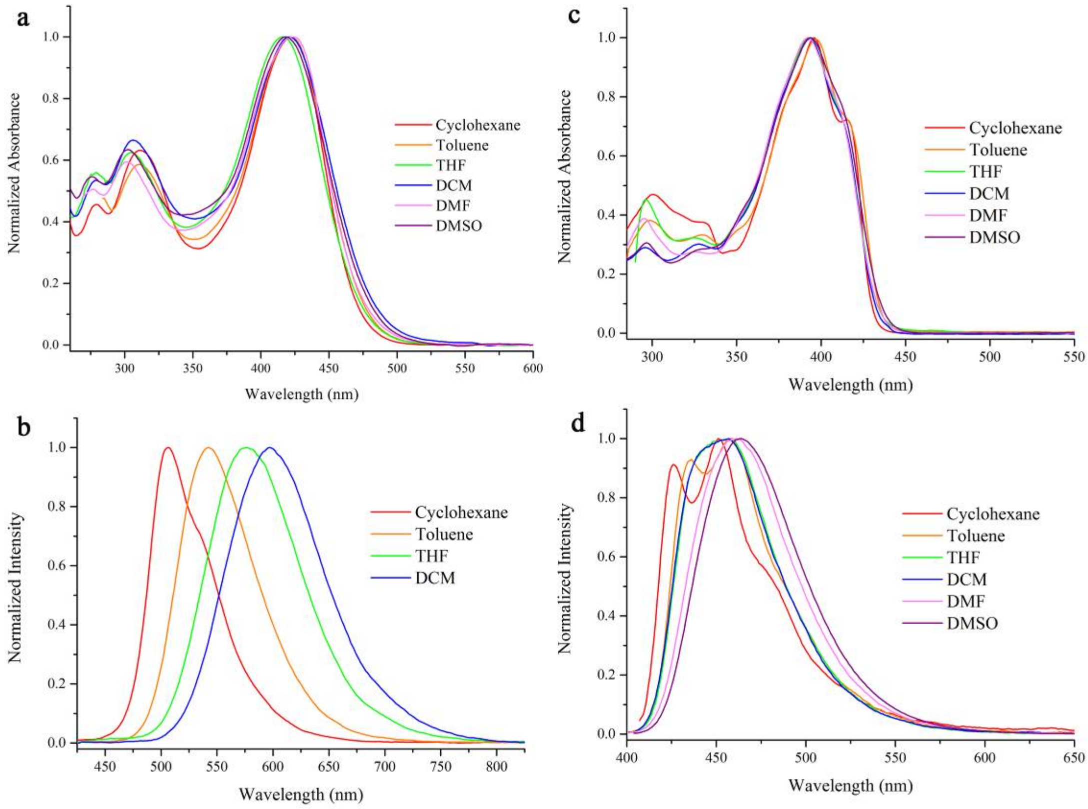

Figure S1. Normalized UV-vis spectra of **P16B** (a) and **P16OB** (c) and normalized fluorescent emission spectra of **P16B** (b, excited at 420 nm) and **P16OB** (d, excited at 395 nm) in different solvents (1.0×10^{-5}mol/L).

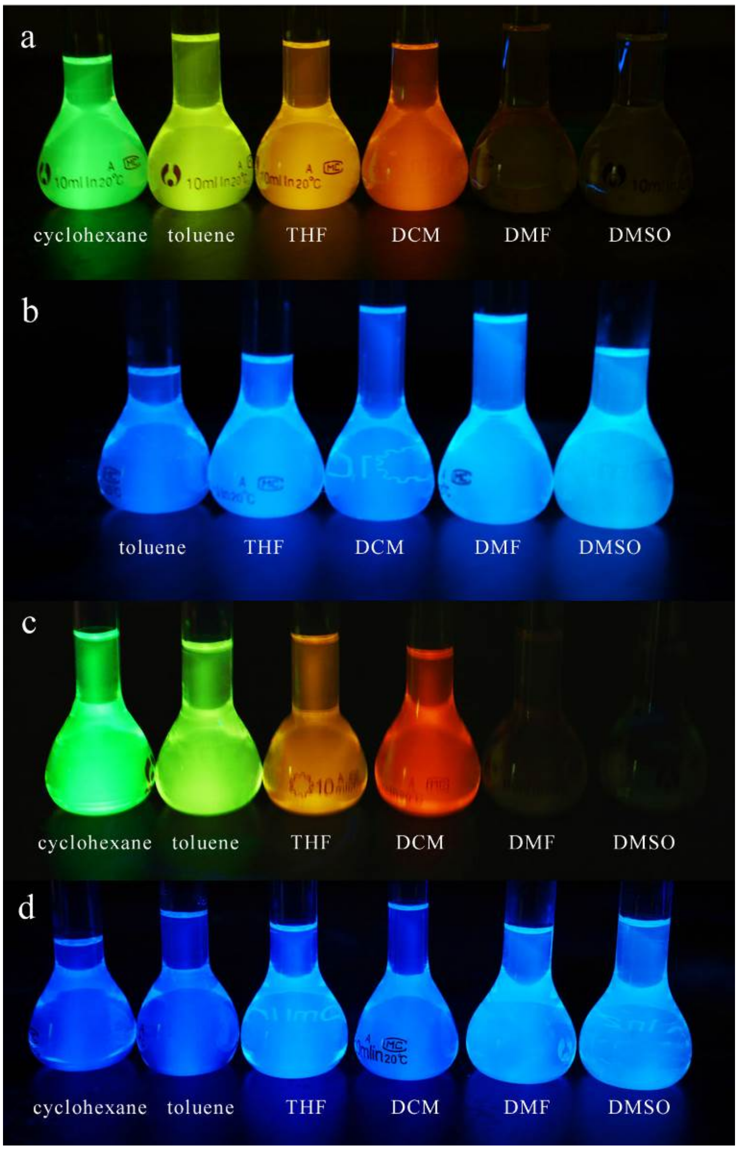

Figure S2. Photos of **P2B** (a), **P2OB** (b), **P16B** (c) and **P16OB** (d) in different solvents under UV light.

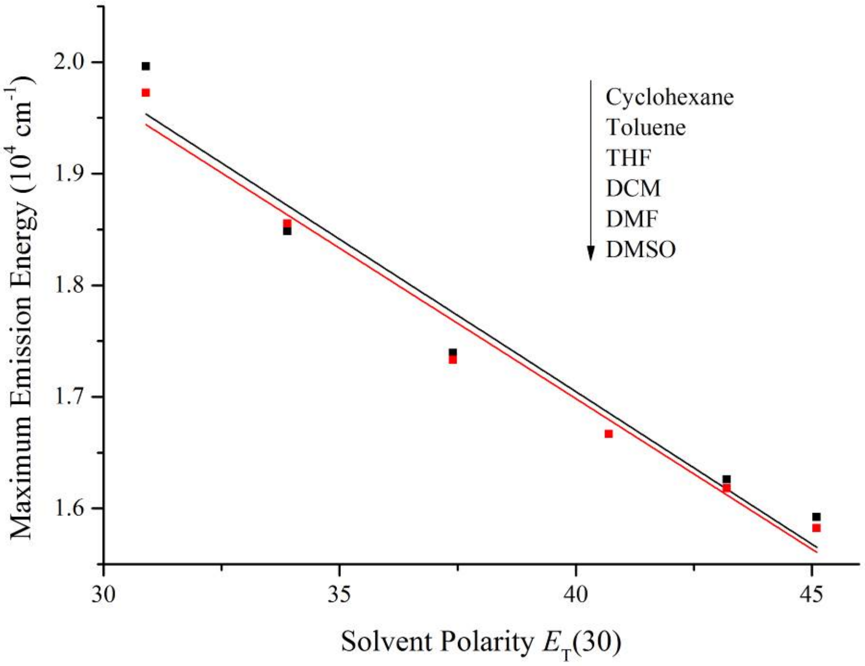

Figure S3. The plots for the maximum fluorescence emission energy of **P2B** (black) and **P16B** (red) *vs* the solvent polarity.

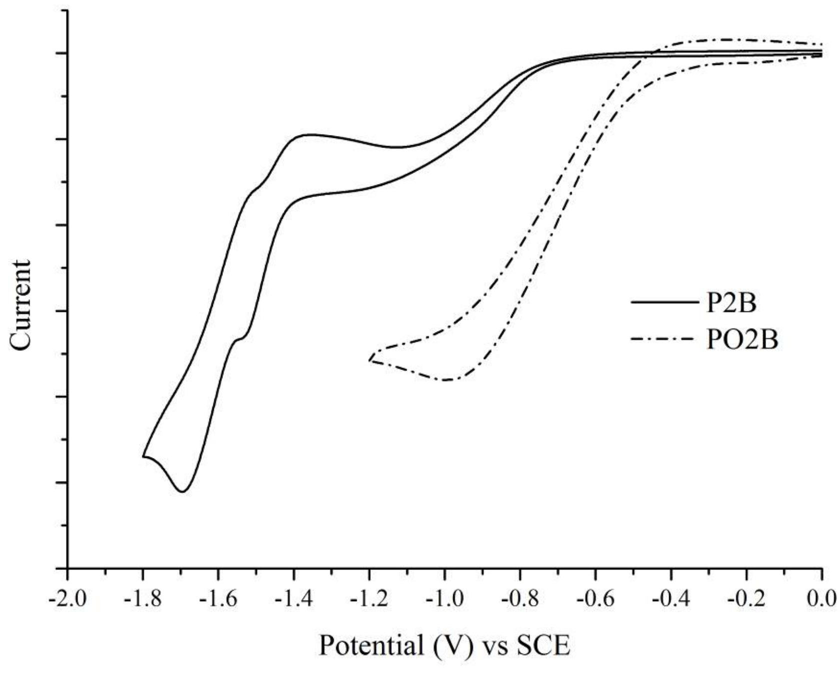

Figure S4. Cyclic voltammograms of **P2B** and **PO2B** measured in CH_2Cl_2 with Bu_4NBF_4 (0.1 M) as electrolyte at a scan rate of 50 mV/s .

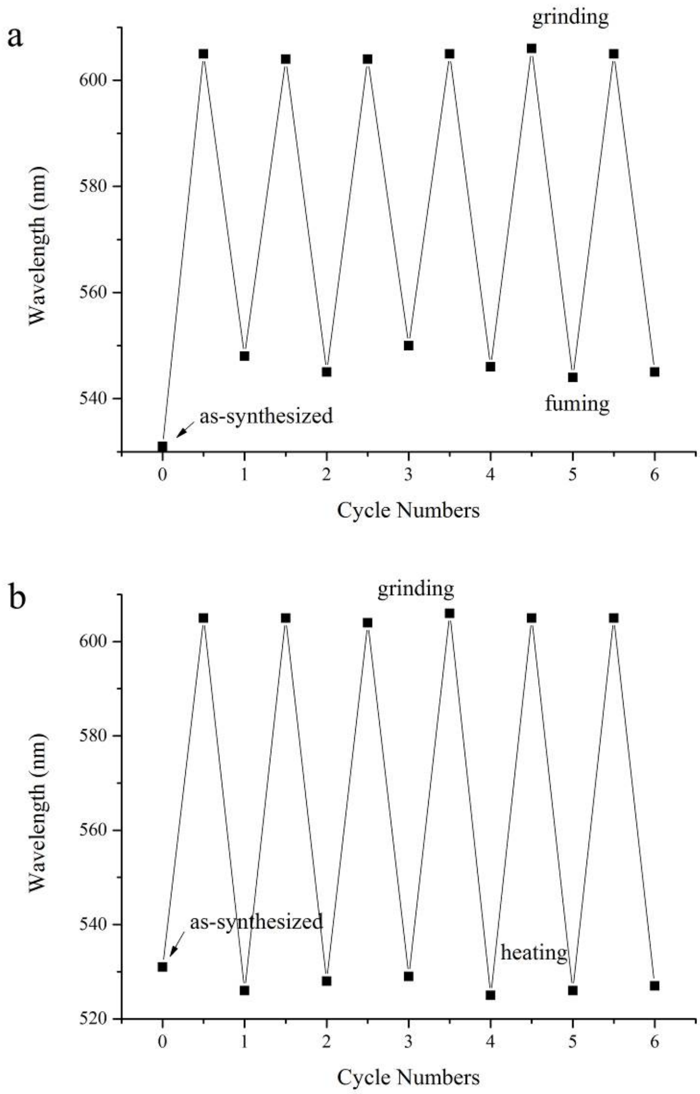

Figure S5. Maximum fluorescent emission of **P2B** upon treated by repeating grinding and fuming with DCM for 5 s (a), or heating at 160 °C for 3 s (b), respectively.

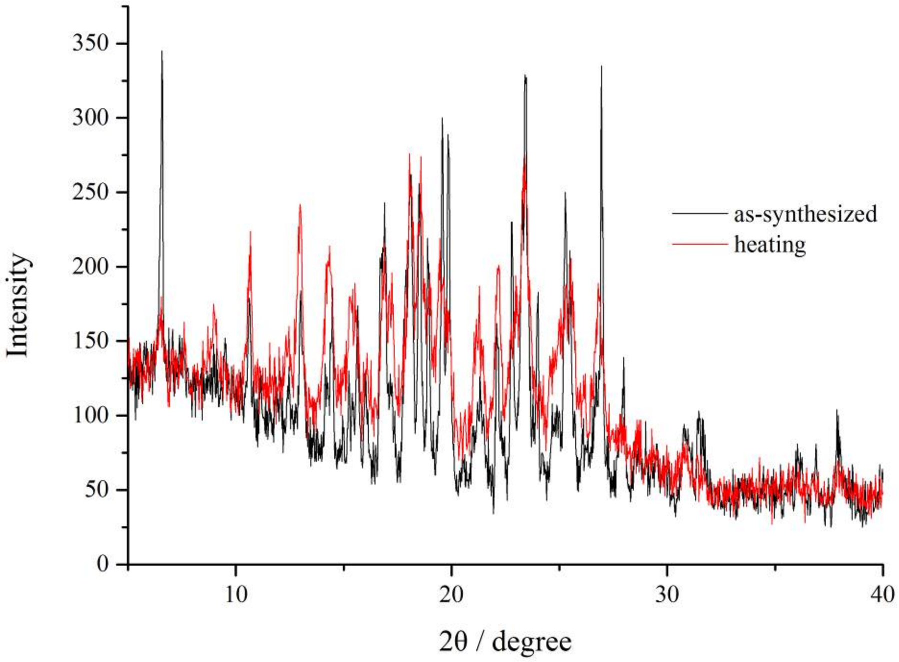

Figure S6. XRD patterns of **P2B** in the as-synthesized crystals and the heated samples.

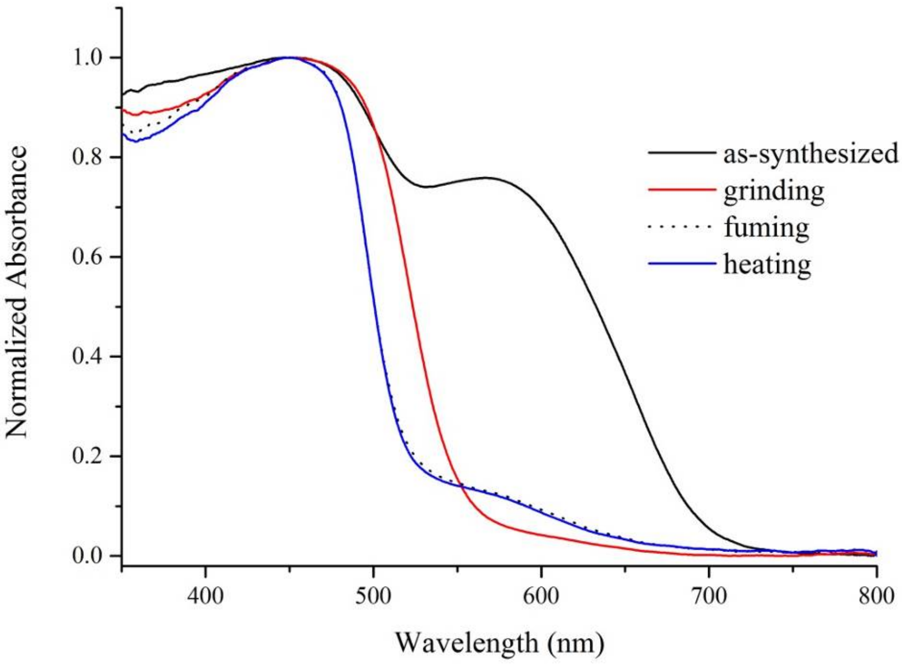

Figure S7. UV-vis spectra of **P2B** in different solid states measured in a reflection mode.

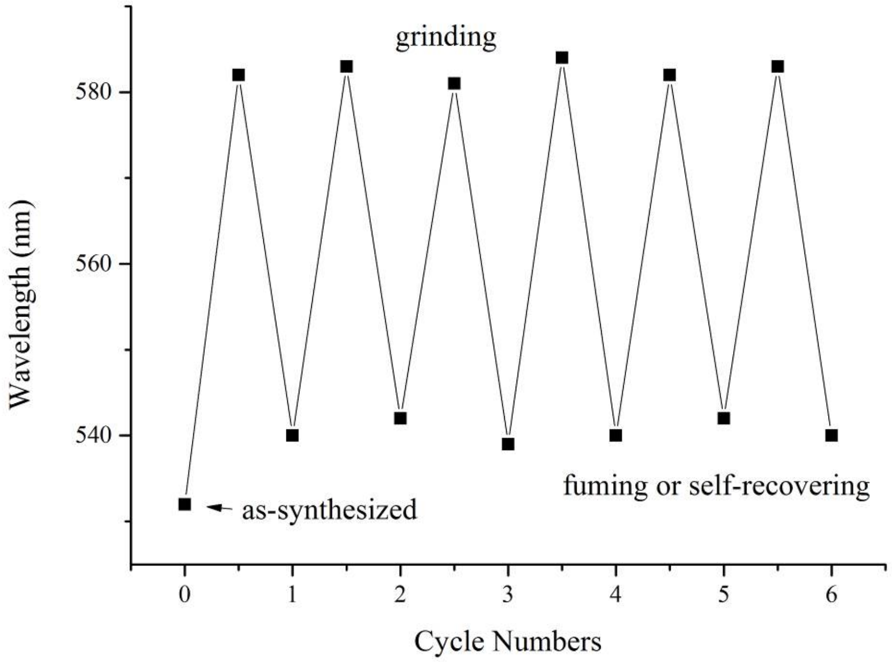

Figure S8. Maximum fluorescent emission of **P16B** upon treated by repeating grinding and fuming with DCM or self-recovering.

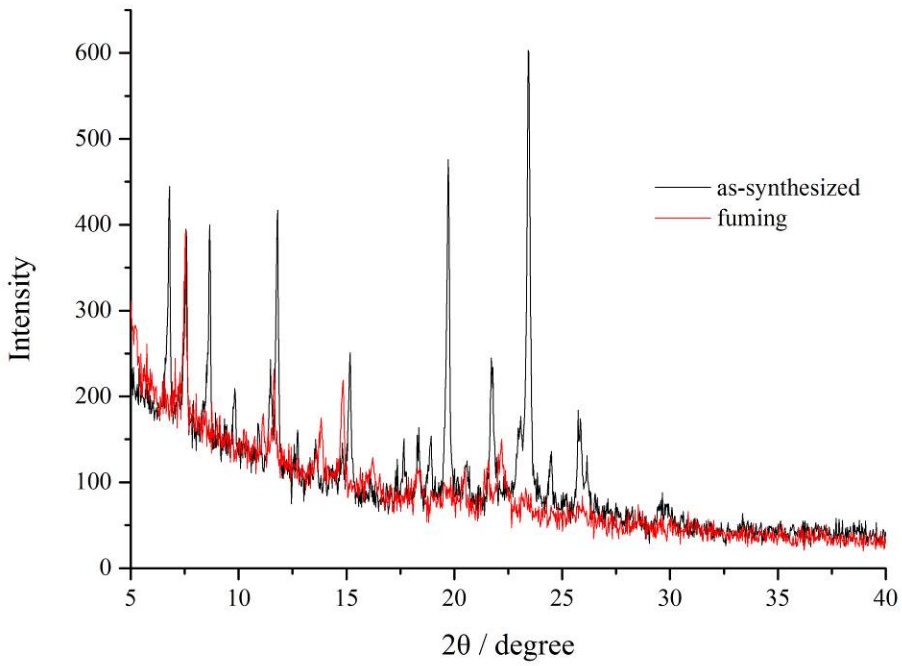

Figure S9. XRD patterns of **P16B** in the as-synthesized crystals and the fumed samples.

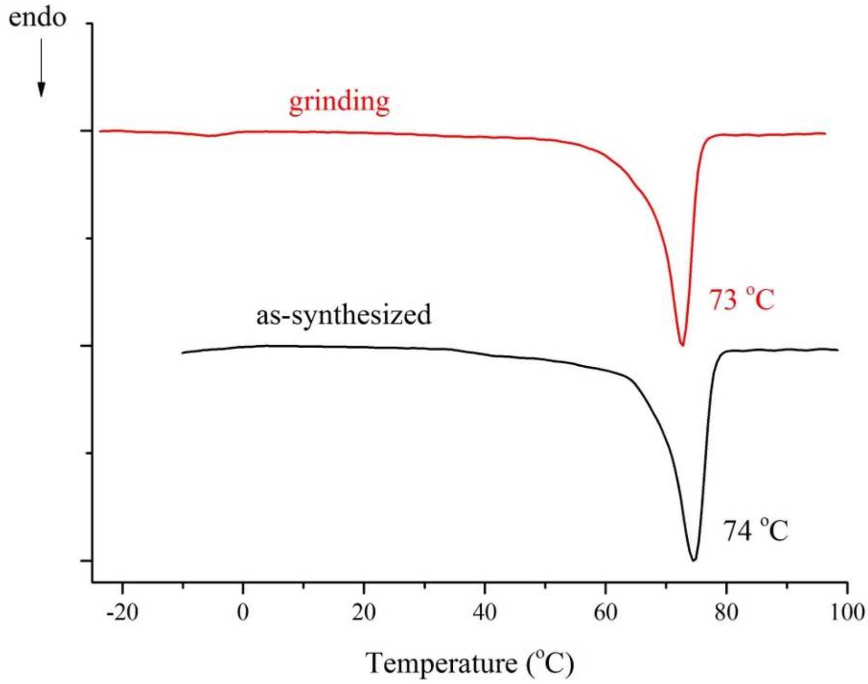

Figure S10. DSC curves of **P16B** in as-synthesized crystals (black) and in ground powders (red).

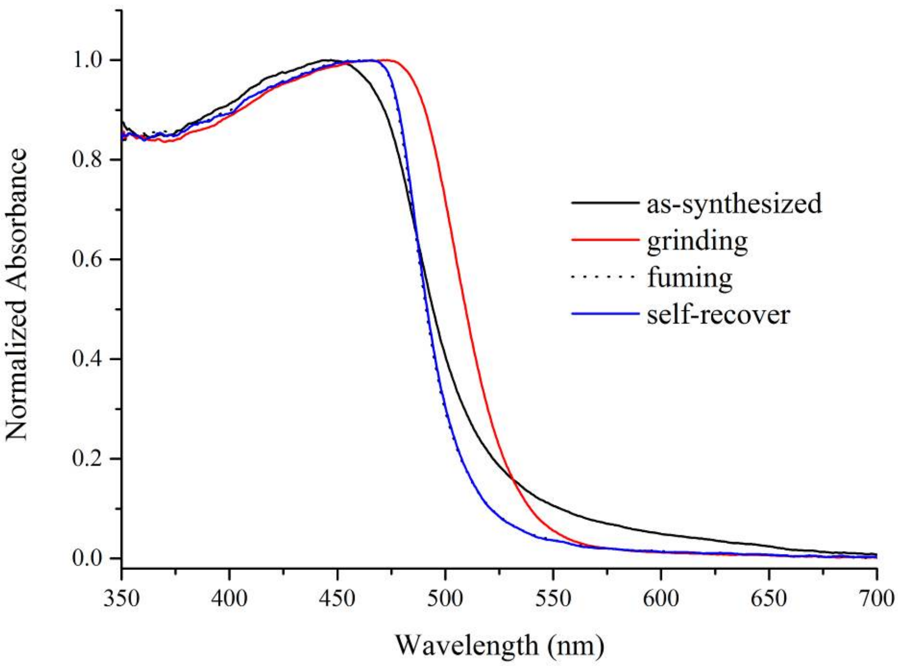

Figure S11. UV-vis spectra of **P16B** in different solid states measured in a reflection mode.

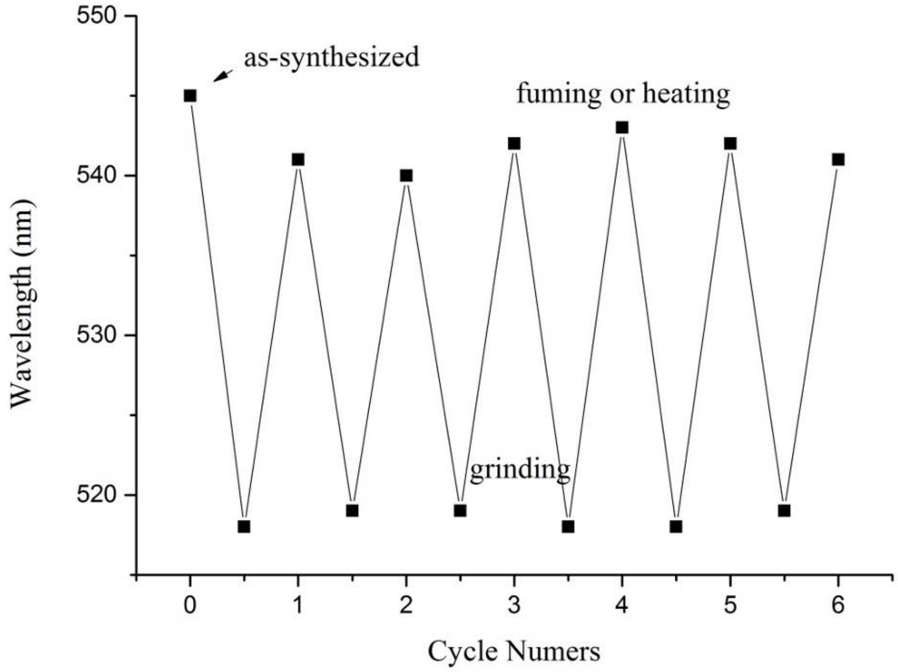

Figure S12. Maximum fluorescent emission of **PO2B** upon treated by repeating grinding and fuming by DCM or heating at 160 ^{o}C.

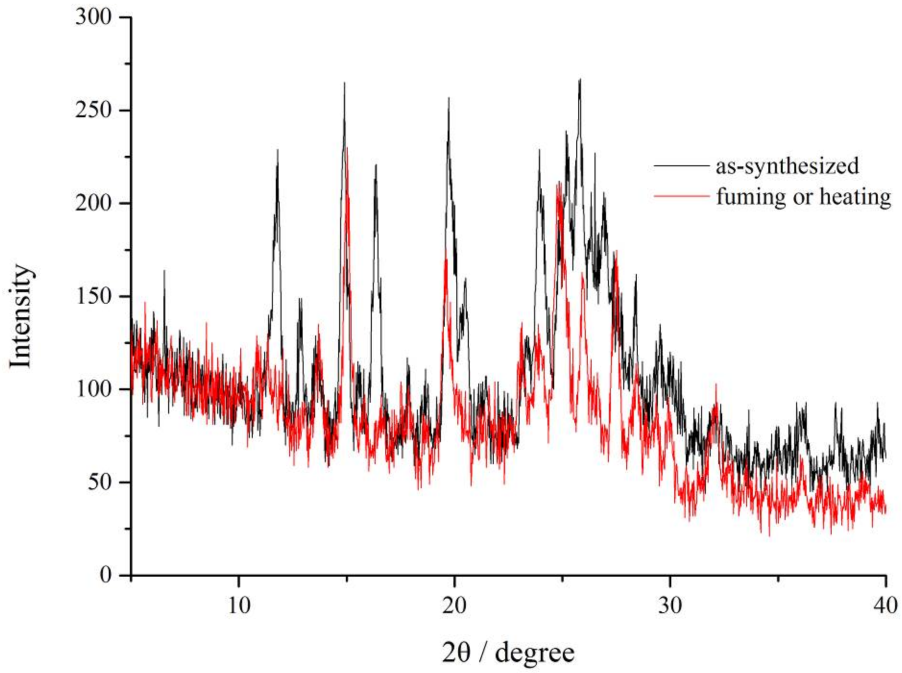

Figure S13. XRD patterns of **PO2B** in the as-synthesized crystals and the fumed/heated samples.

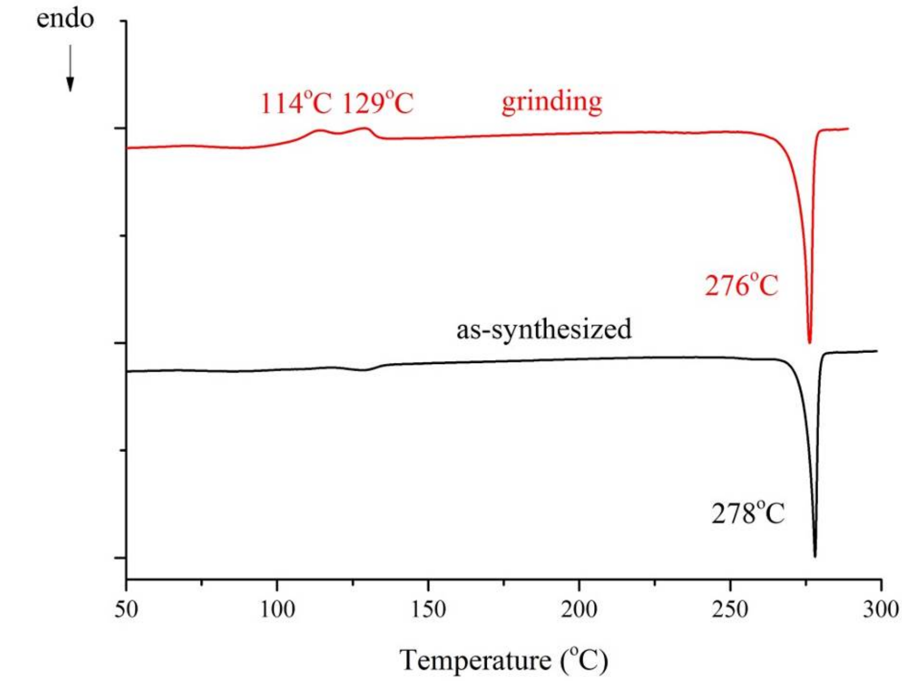

Figure S14. DSC curves of **PO2B** in as-synthesized crystals (black) and in ground powders (red).

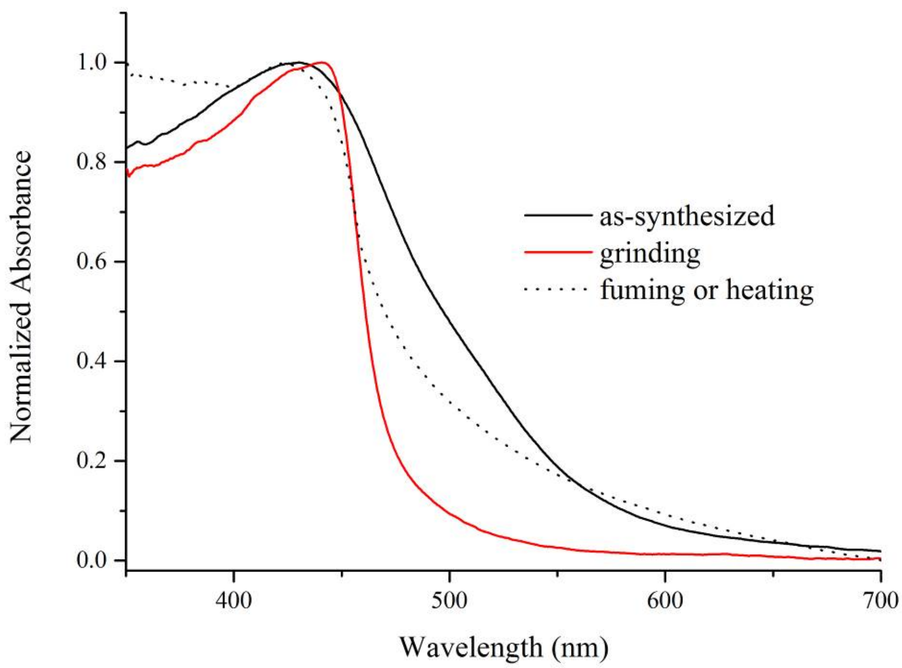

Figure S15. UV-vis spectra of **PO2B** in different solid states measured in a reflection mode.

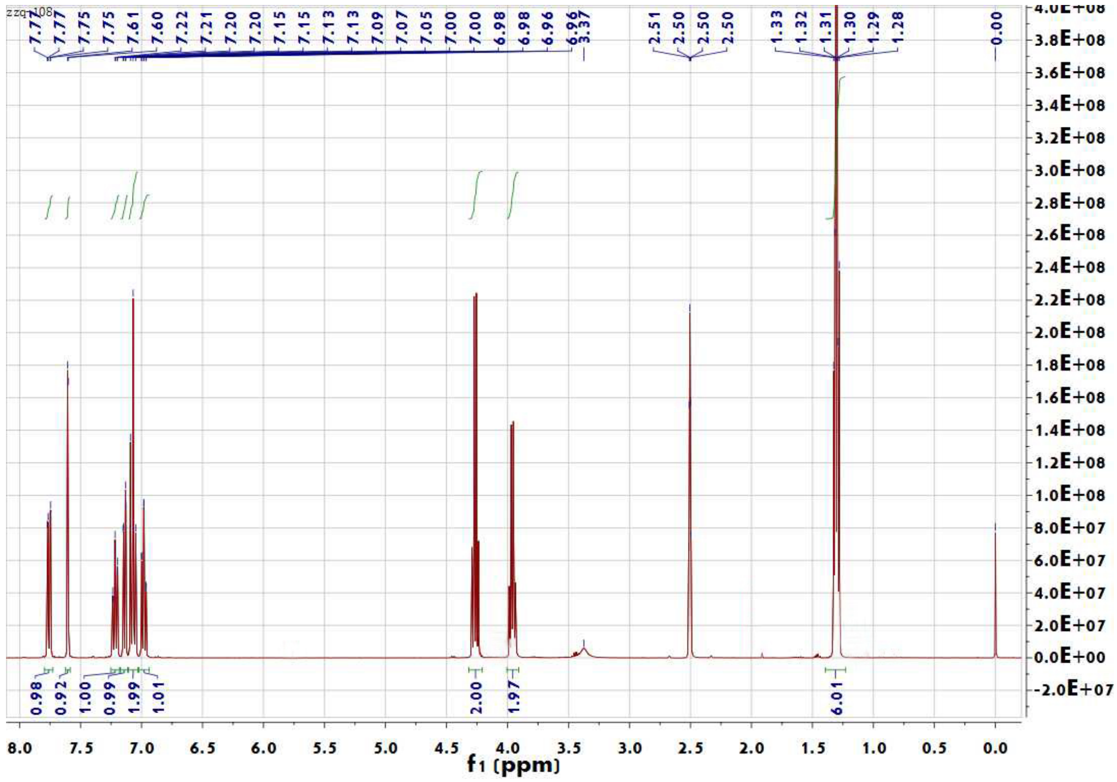

Figure S16. ^{1}H NMR (400 MHz) spectrum of compound **2a** in DMSO-d_6.

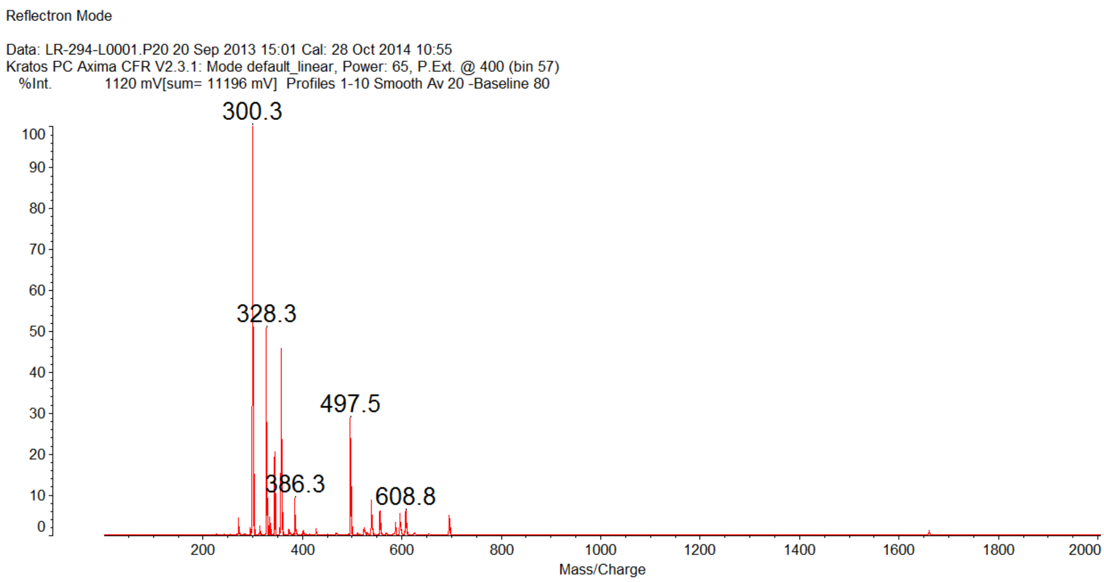

Figure S17. MALDI/TOF MS spectrum of compound **2a**.

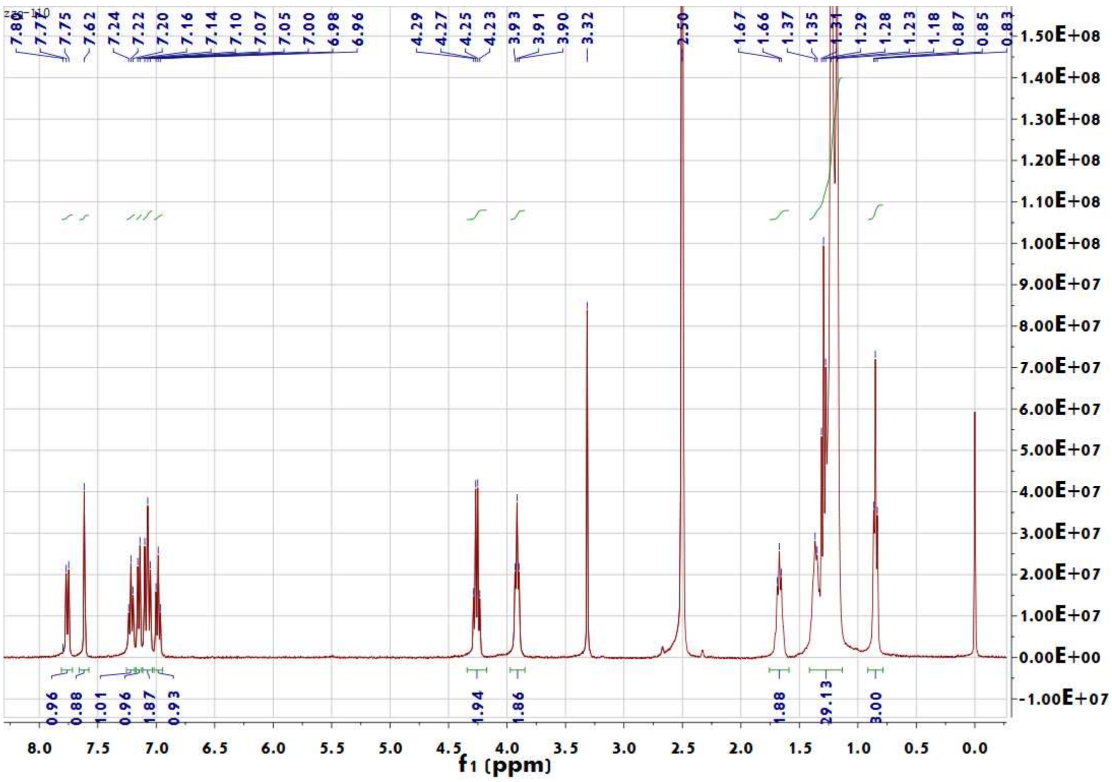

Figure S18. ^{1}H NMR (400 MHz) spectrum of compound **2b** in DMSO-d_6.

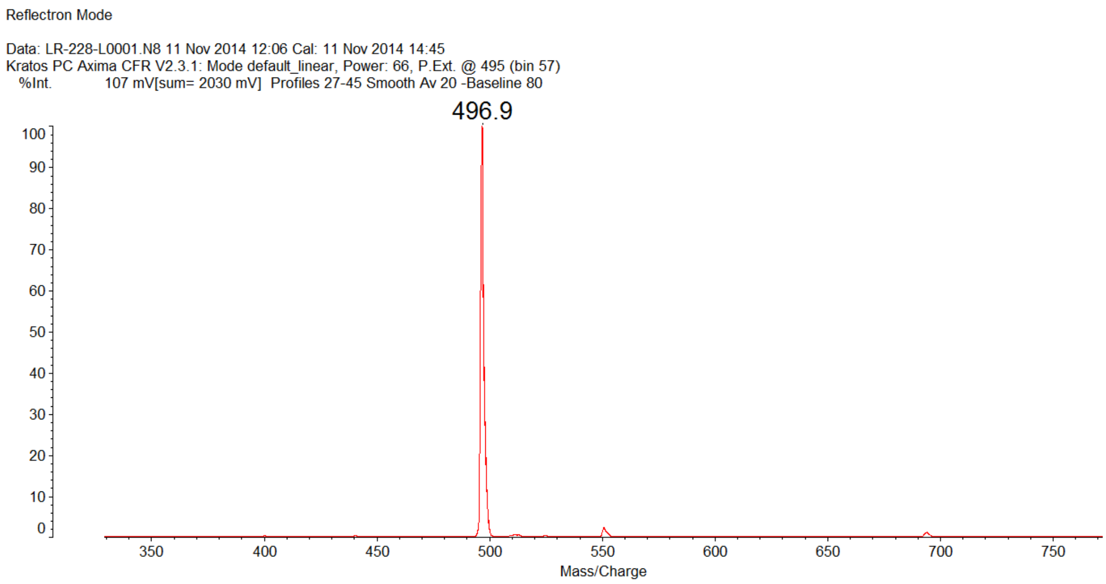

Figure S19. MALDI/TOF MS spectrum of compound **2b**.

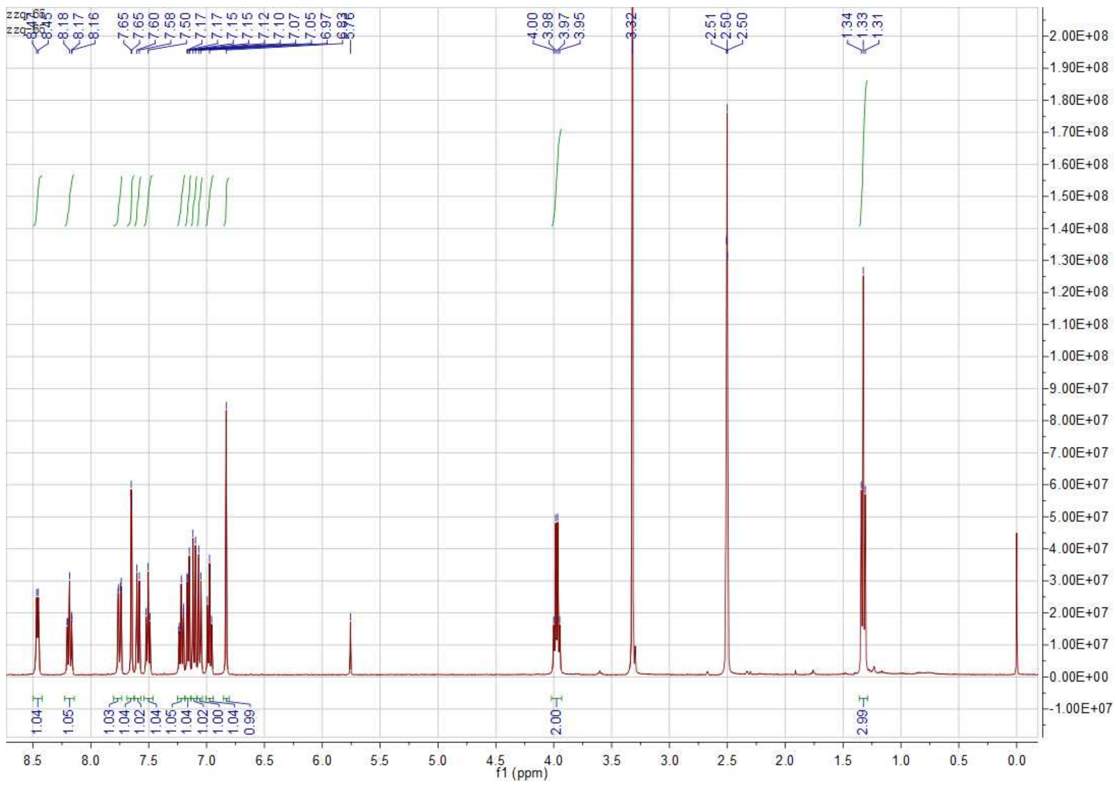

Figure S20. [1]H NMR (400 MHz) spectrum of compound **P2B** in DMSO-d_6.

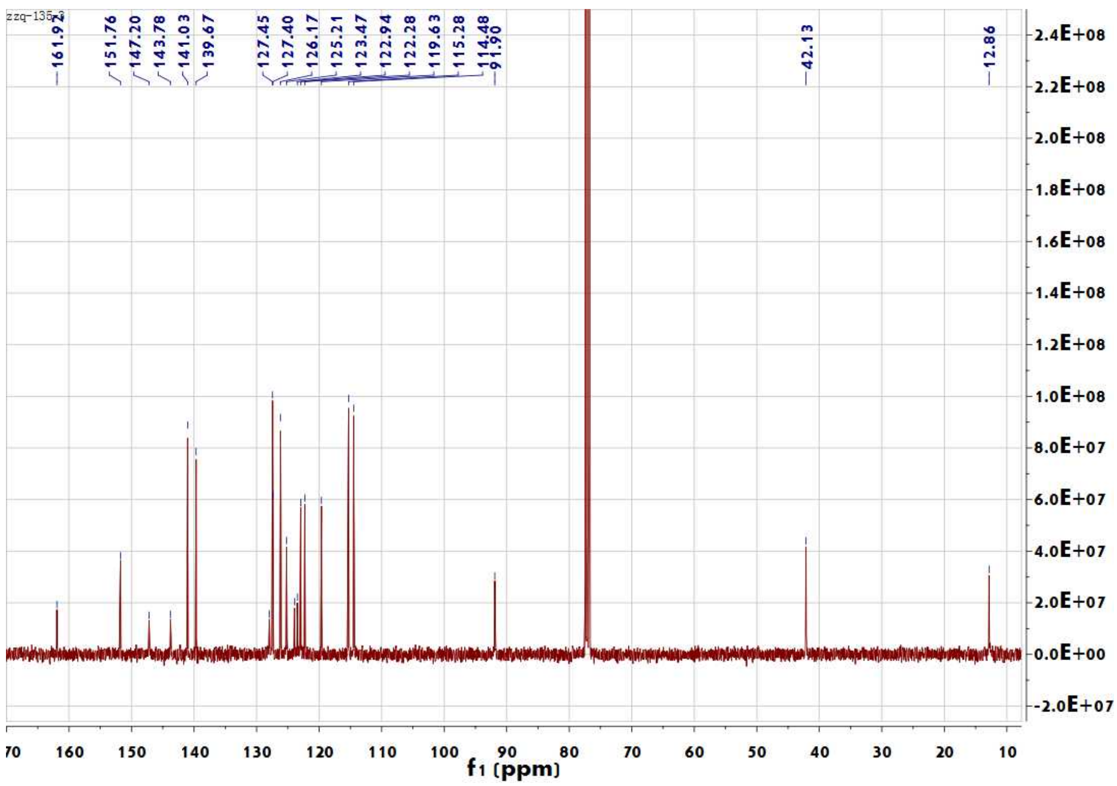

Figure S21. [13]C NMR (100 MHz) spectrum of compound **P2B** in $CDCl_3$.

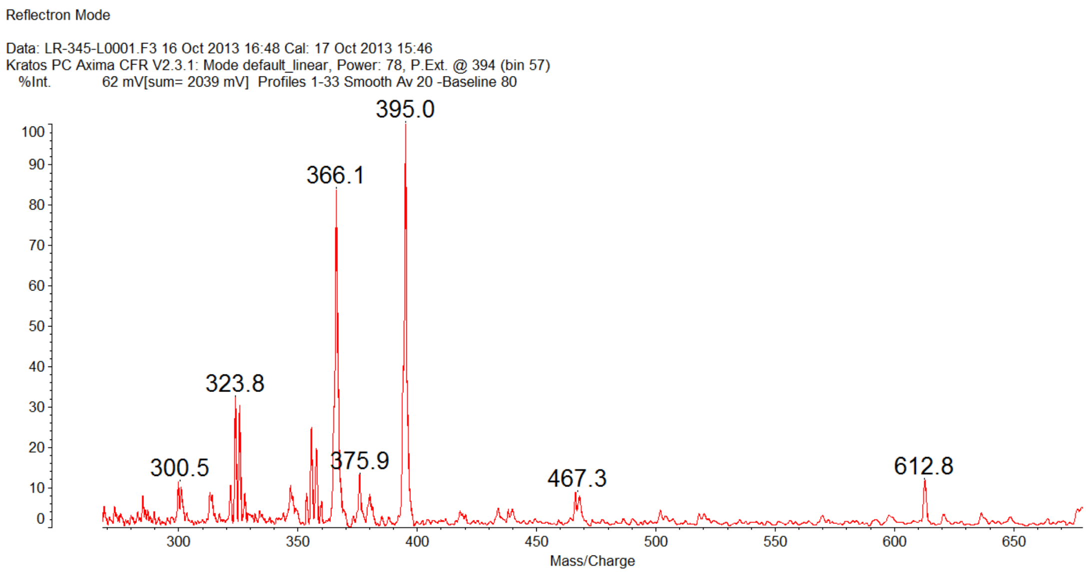

Figure S22. MALDI/TOF MS spectrum of compound **P2B**.

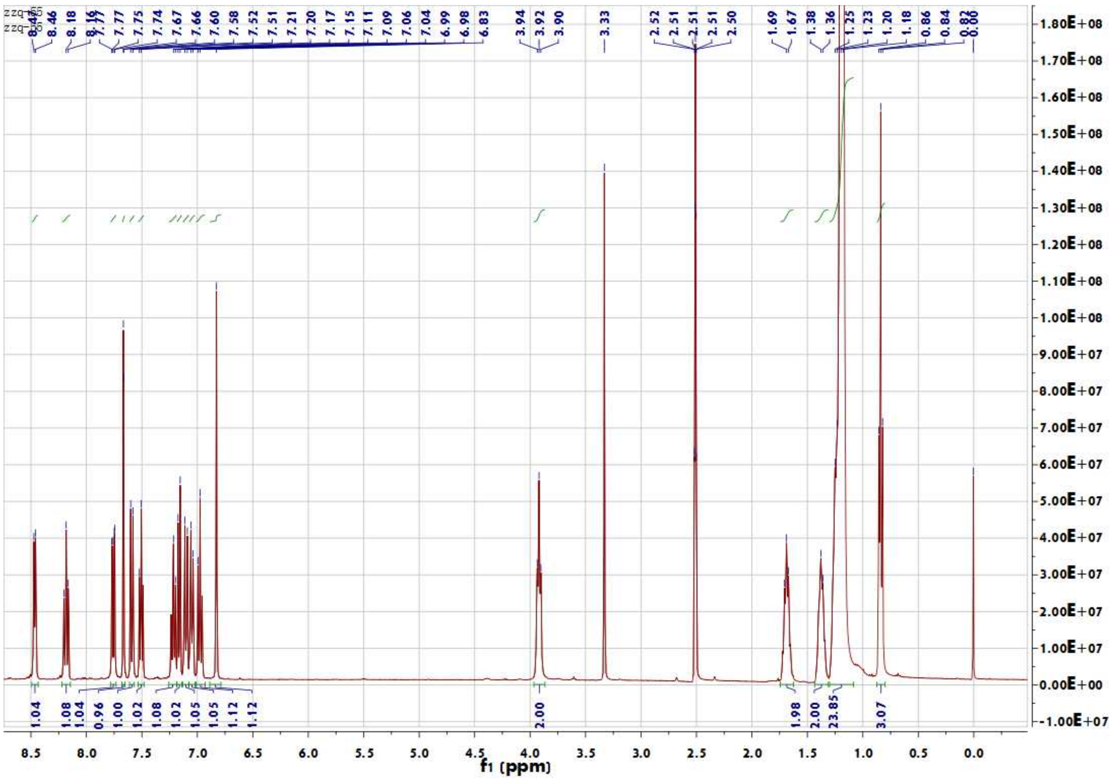

Figure S23. [1]H NMR (400 MHz) spectrum of compound **P16B** in DMSO-d_6.

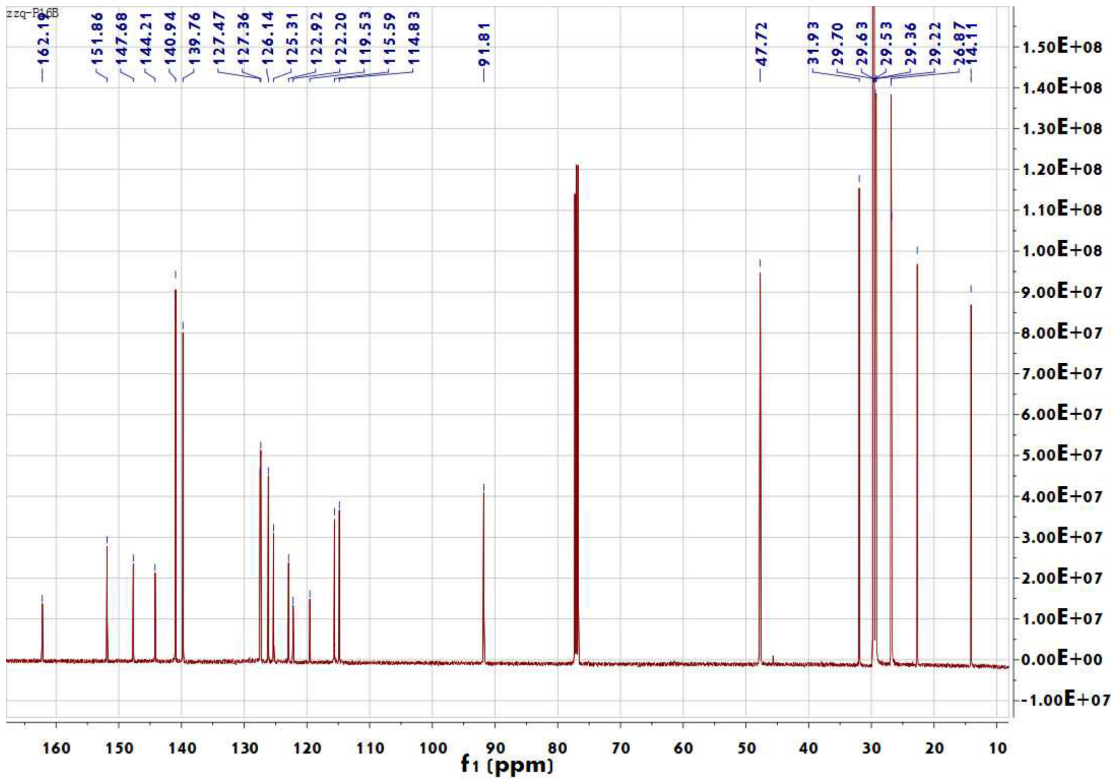

Figure S24. ^{13}C NMR (125 MHz) spectrum of compound **P16B** in $CDCl_3$.

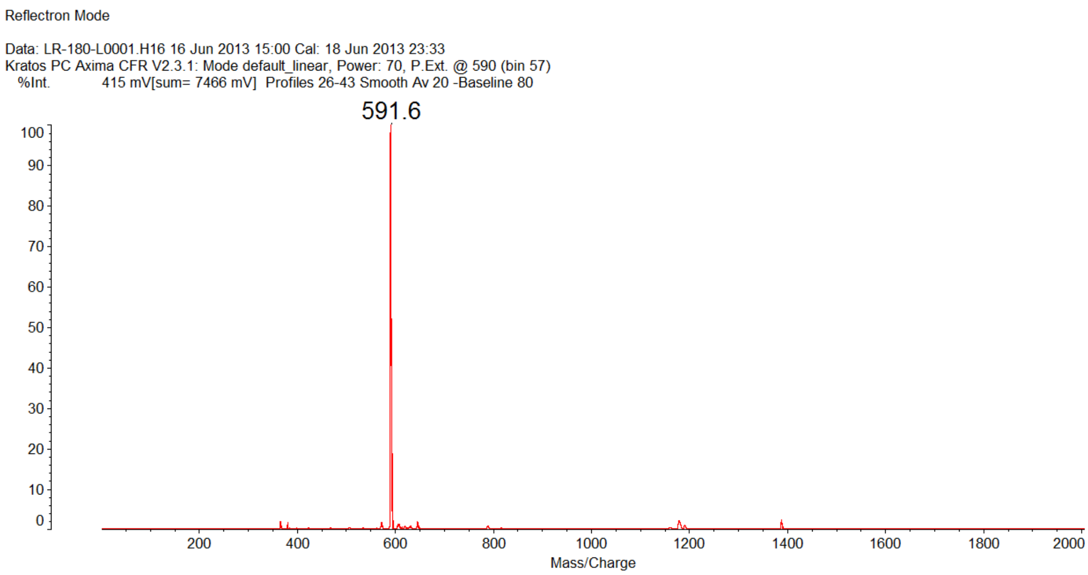

Figure S25. MALDI/TOF MS spectrum of compound **P16B**.

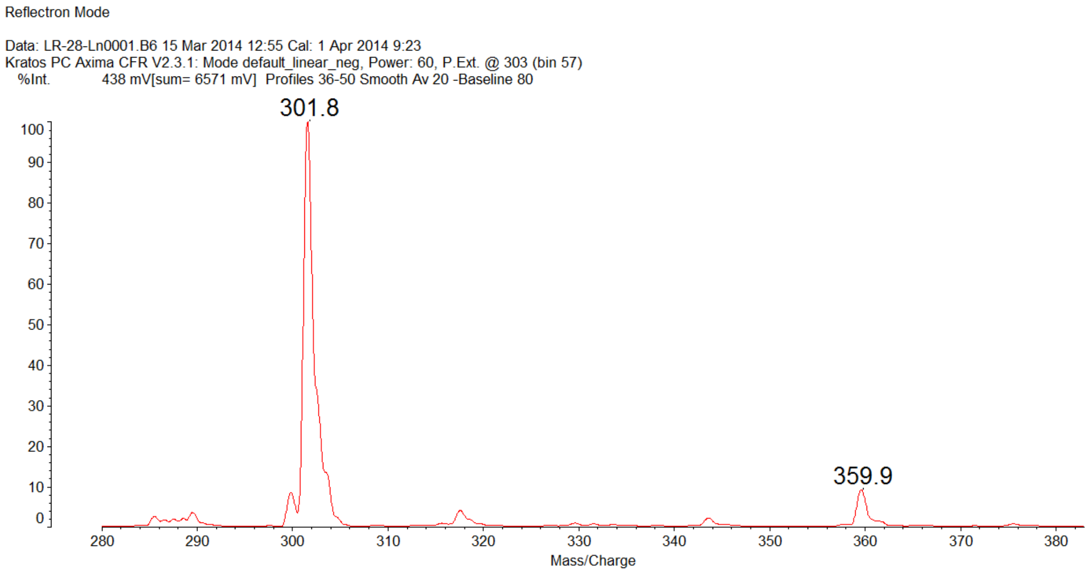

Figure S26. MALDI/TOF MS spectrum of compound **4a**.

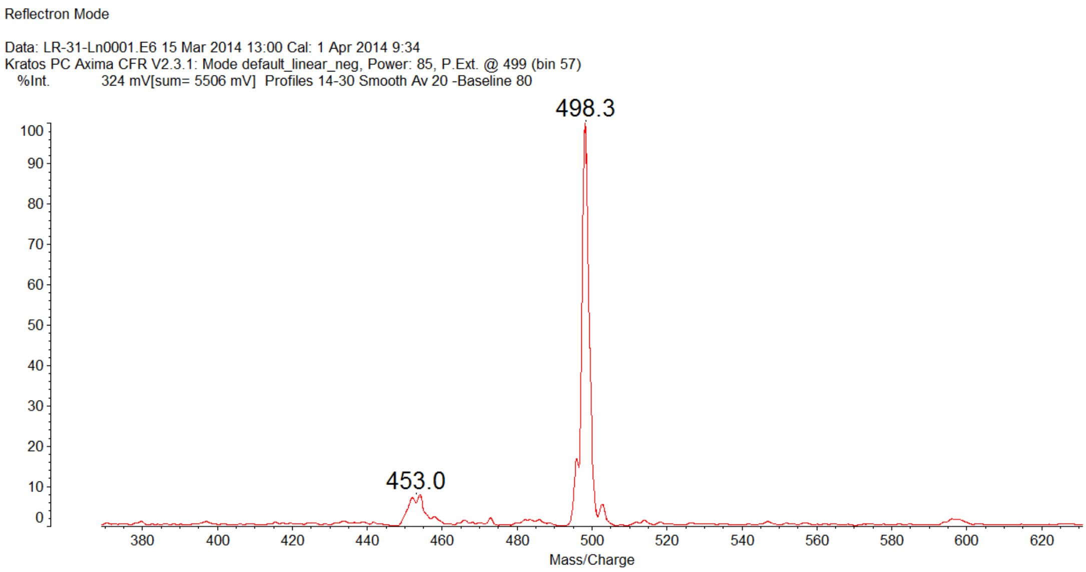

Figure S27. MALDI/TOF MS spectrum of compound **4b**.

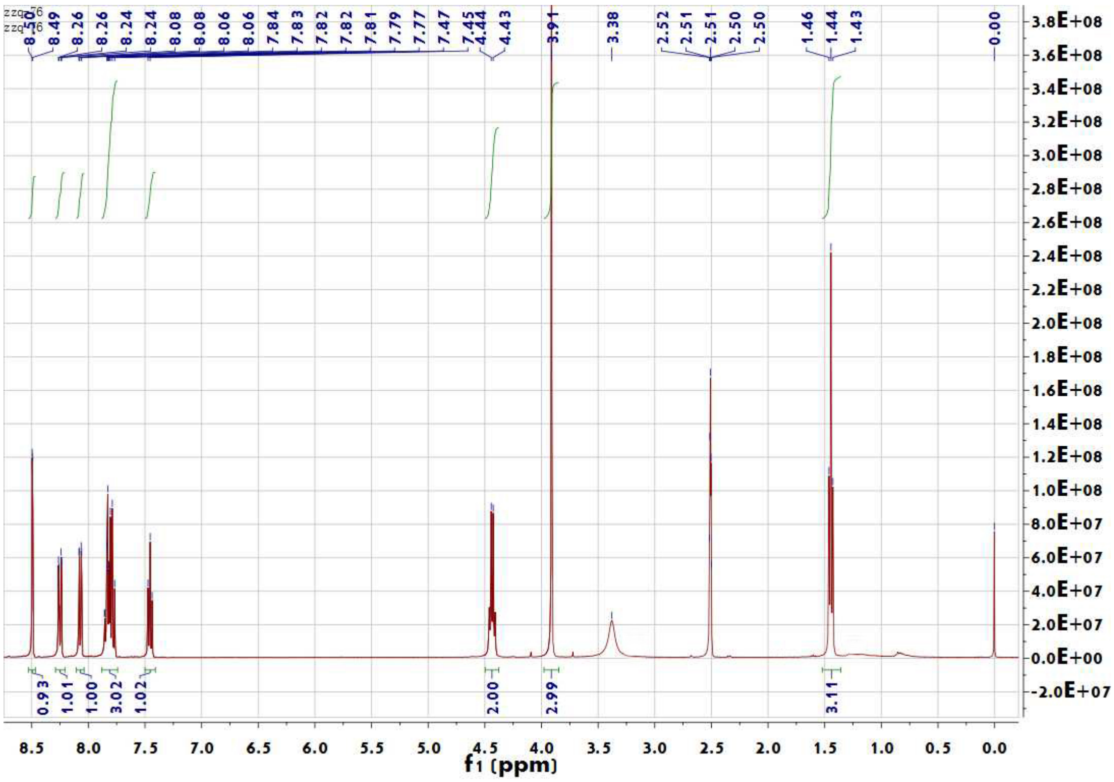

Figure S28. [1]H NMR (400 MHz) spectrum of compound **5a** in DMSO-d_6.

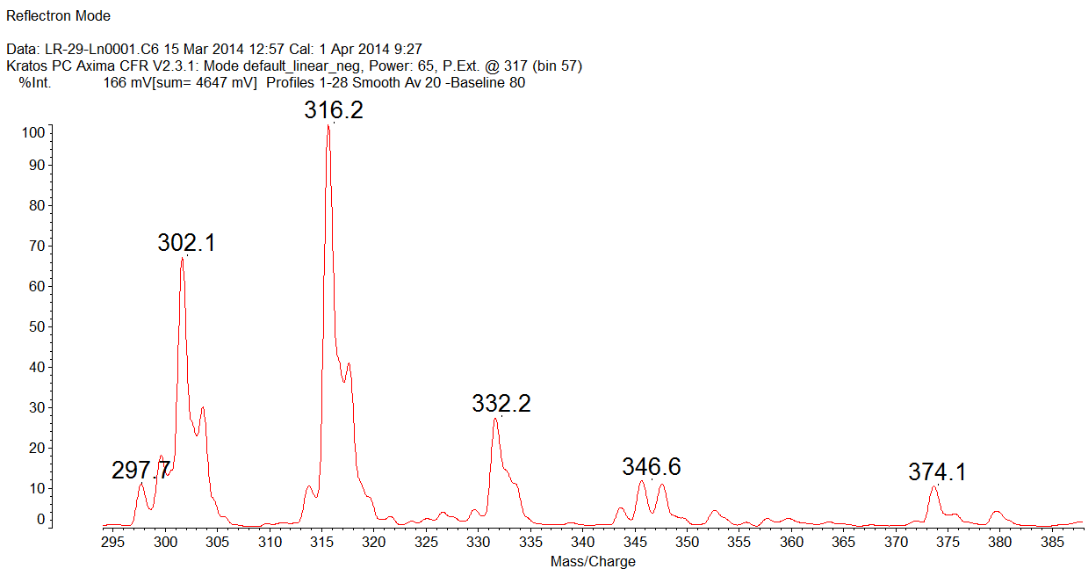

Figure S29. MALDI/TOF MS spectrum of compound **5a**.

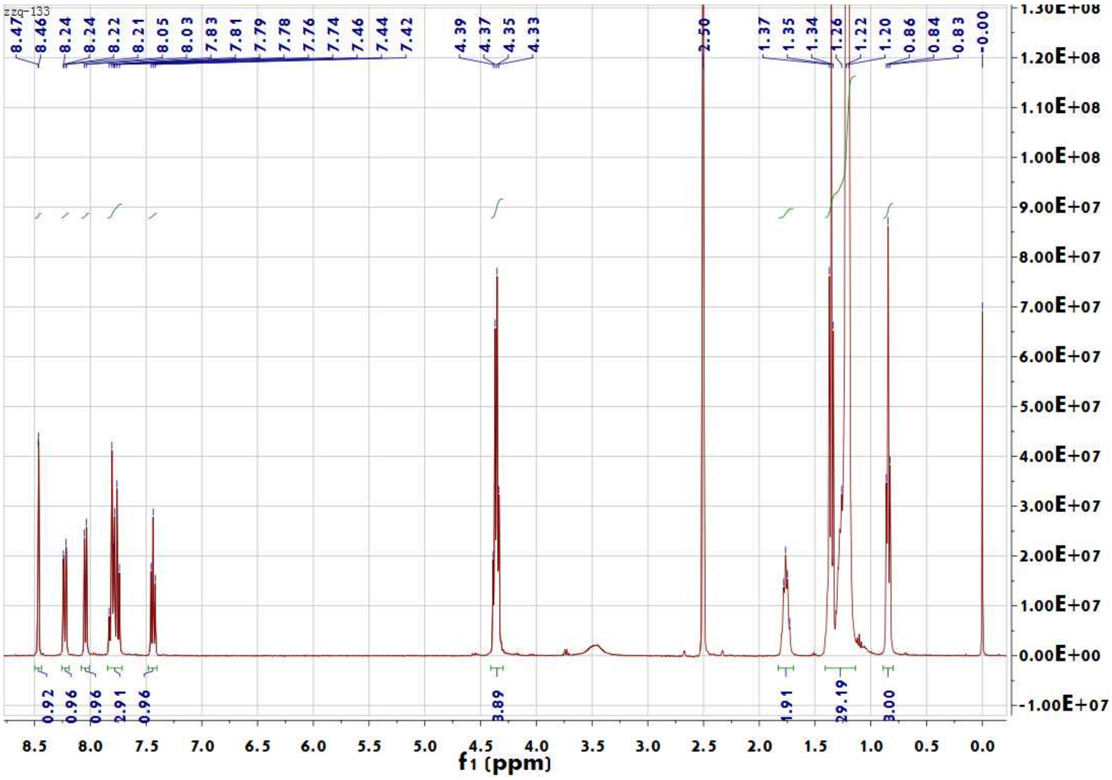

Figure S30. [1]H NMR (400 MHz) spectrum of compound **5b** in DMSO-d_6.

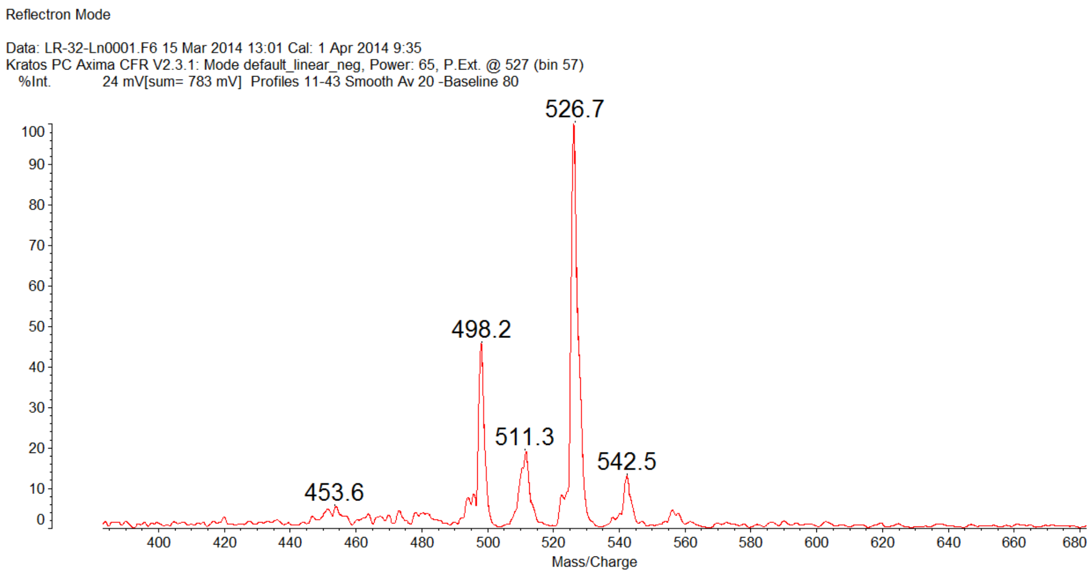

Figure S31. MALDI/TOF MS spectrum of compound **5b**.

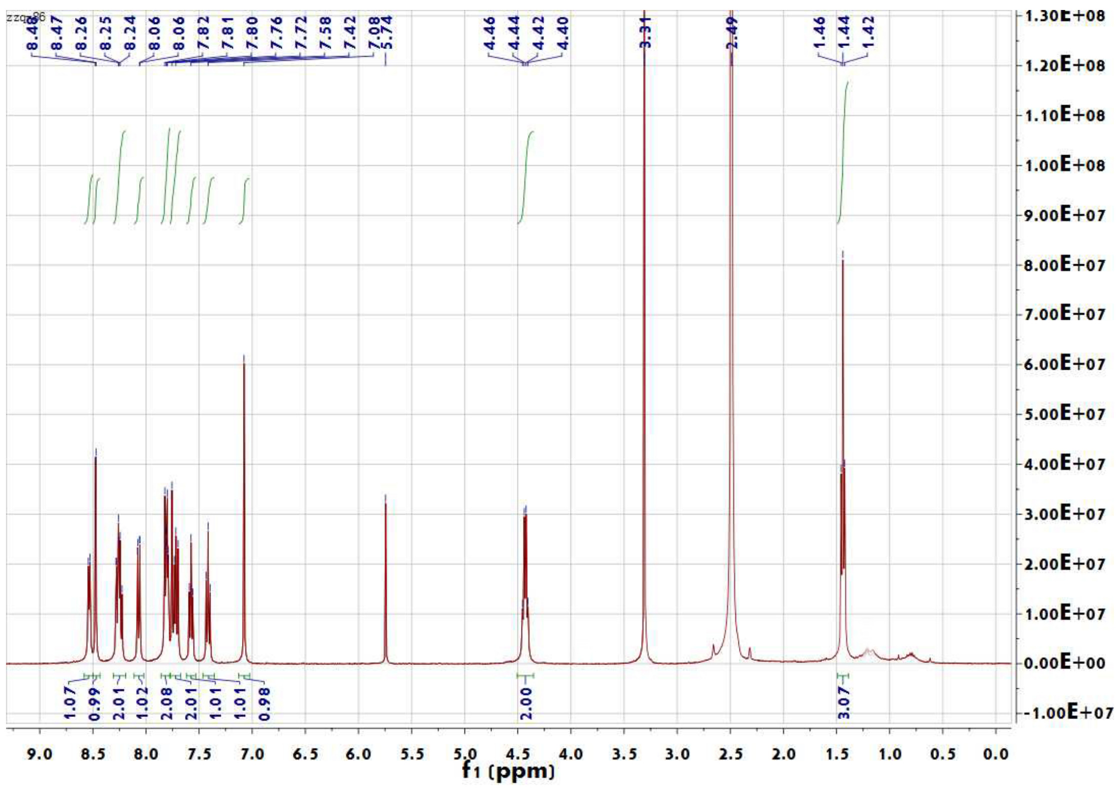

Figure S32. [1]H NMR (400 MHz) spectrum of compound **PO2B** in DMSO-d_6.

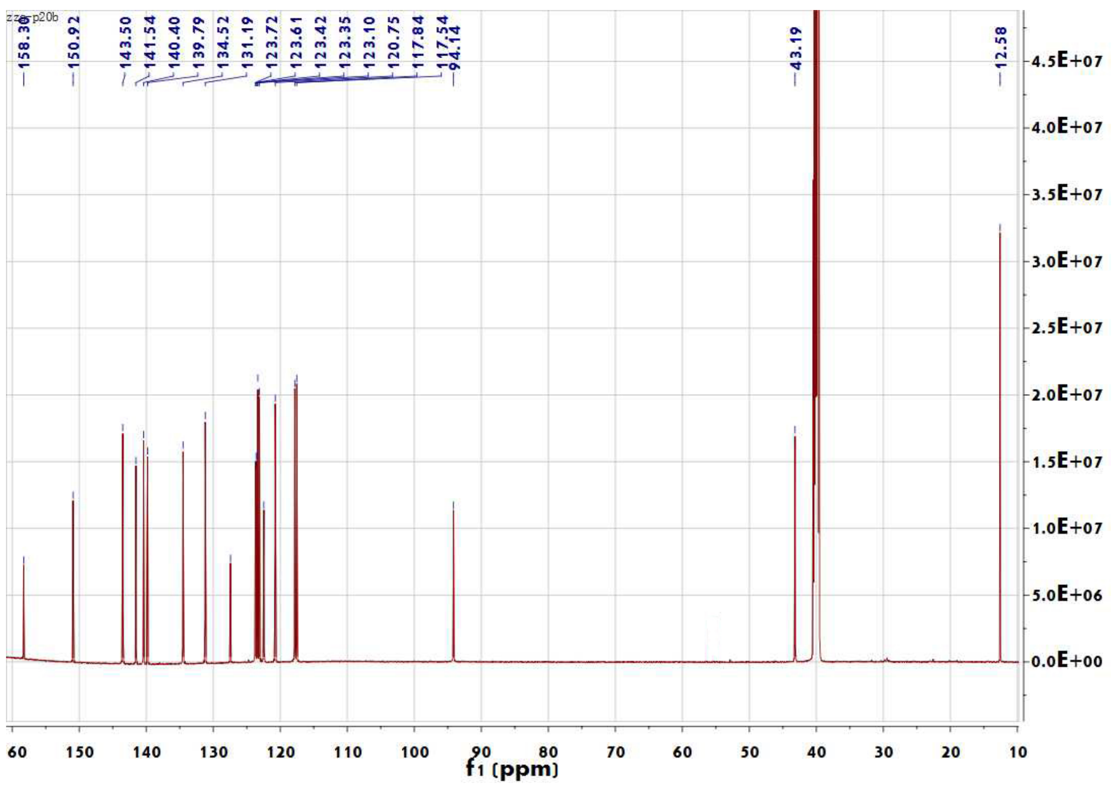

Figure S33. [13]C NMR (125 MHz) spectrum of compound **PO2B** in DMSO-d_6.

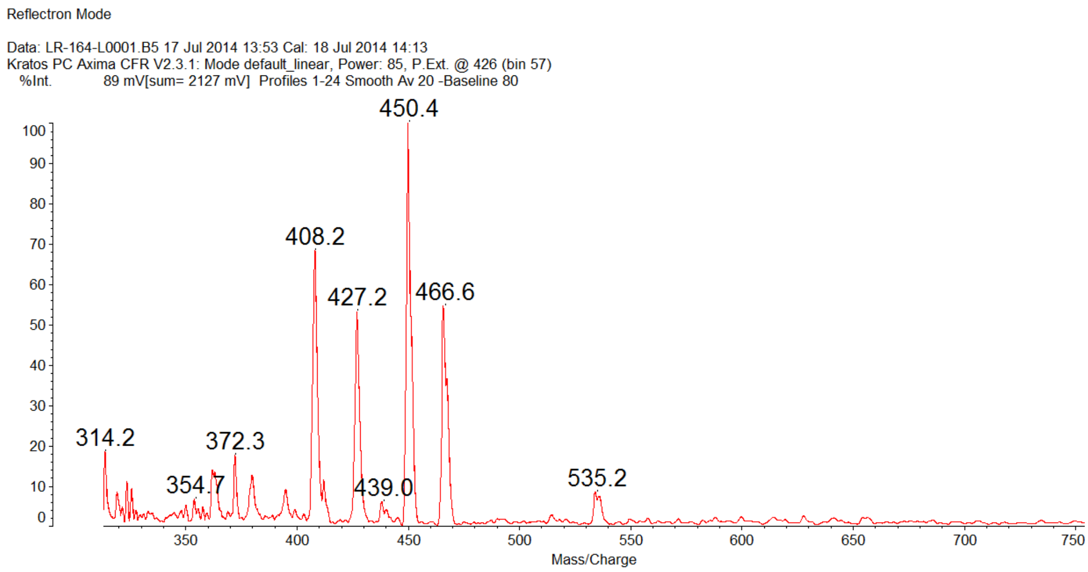

Figure S34. MALDI/TOF MS spectrum of compound **PO2B**.

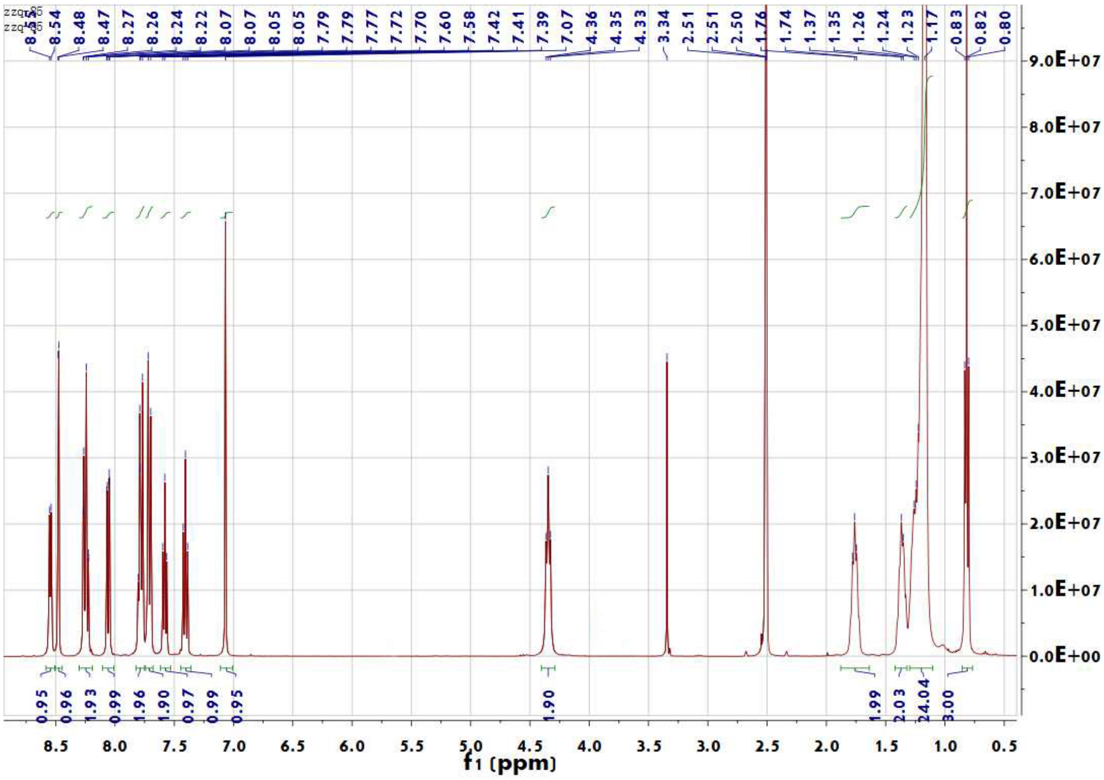

Figure S35. [1]H NMR (400 MHz) spectrum of compound **PO16B** in DMSO-d_6.

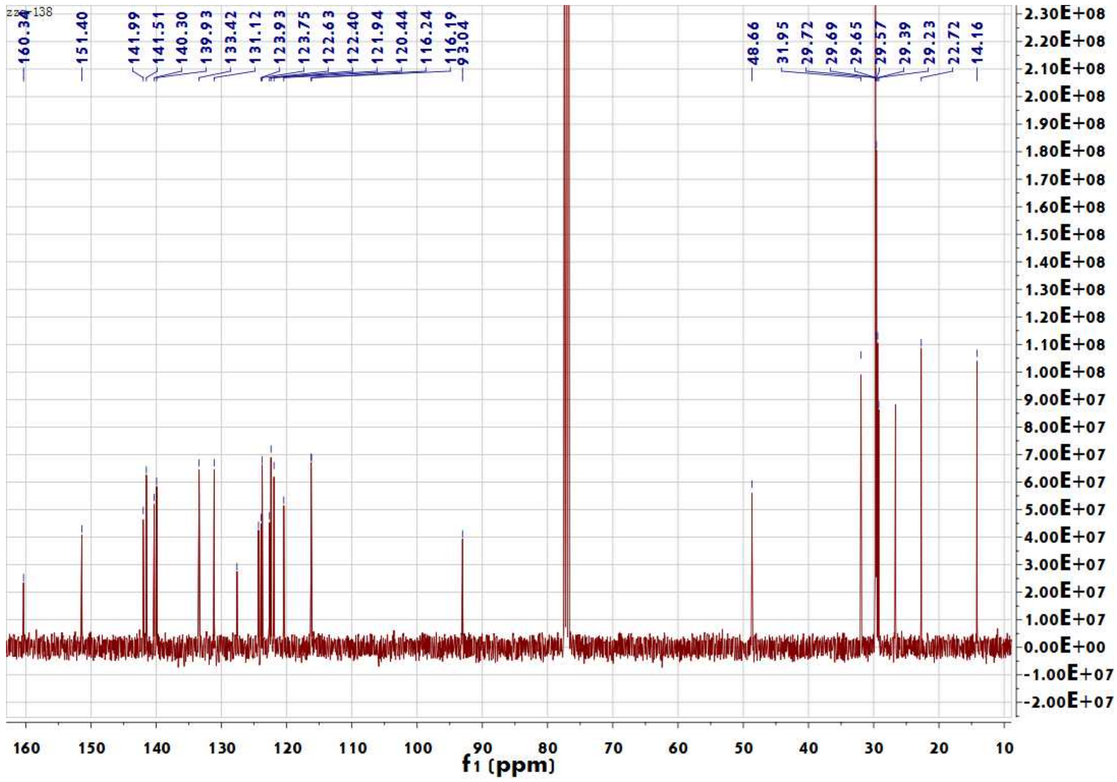

Figure S36. ^{13}C NMR (100 MHz) spectrum of compound **PO16B** in $CDCl_3$.

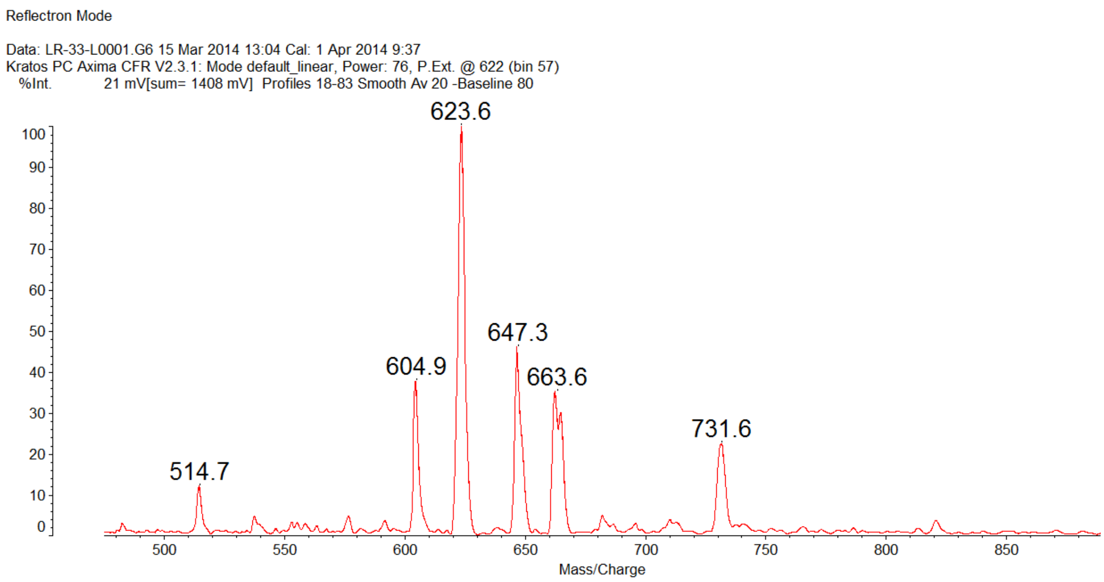

Figure S37. MALDI/TOF MS spectrum of compound **PO16B**.